Structural and Magnetic Properties of Co-Fe Binary Alloy Monolayers on W(110)

M. Pratzer and H. J. Elmers

Institut für Physik, Johannes Gutenberg–Universität Mainz, Staudingerweg 7, D-55099 Mainz, Germany

(Received 21 October 2002; published 19 February 2003)

We present an experimental investigation of $\mathrm{Co}_x\mathrm{Fe}_{1-x}$ monolayers grown on flat and stepped W(110) surfaces. Atomically resolved scanning tunneling microscopy and low energy electron diffraction reveal continuous miscibility and pseudomorphic growth of Co and Fe for $0 \leq x < 0.6$. We observe short range ordered CoFe_3-$p(2 \times 2)$ and CoFe-$c(2 \times 2)$ structures in the pseudomorphic monolayer. High Co concentrations lead to a phase separation. The Curie temperature and the ferromagnetic Kerr signal at low temperatures decrease monotonically with increasing Co concentration, finally vanishing at $x = 0.5$.

DOI: 10.1103/PhysRevLett.90.077201 PACS numbers: 75.70.Ak, 68.55.Nq, 75.50.Bb

Concerning the magnetic properties of binary transition metal alloys, the most relevant information is given by the Slater-Pauling curve showing a linear increase of the average magnetic moment for early transition metal alloys when plotted as a function of the increasing electron per atom ratio, followed by a linear decrease of the moment when the average d-band occupation increases for the latter transition metal alloys, with a maximum between Fe and Co. In bulk alloys, changes of the effective d-band occupation are inherently related to structural changes [1]. In ultrathin alloy films grown epitaxially on appropriate substrates, the substrate can define the structure independently from the alloy composition [2–4]. Moreover, ultrathin films show surprising and useful magnetic properties deviating from bulk properties even for pure elements [5,6]. This is most pronounced for ferromagnetic monolayer films [7]. The understanding of ferromagnetic order in these two-dimensional systems will substantially improve, when quasi-two-dimensional *monolayers* of ferromagnetic alloys can be prepared.

Accordingly, scientific research has focused on ultrathin epitaxial alloy films. In $\mathrm{Fe}_{1-x}\mathrm{Ni}_x$ alloy films on Cu(100), the fcc phase is stabilized, thus suppressing the Invar effect and revealing a new low-spin phase [2]. For $\mathrm{Co}_x\mathrm{Fe}_{1-x}$ [3] and $\mathrm{Ni}_{1-x}\mathrm{Pd}_x$ [4] alloy films on Cu(100), the fcc phase can be stabilized, also, and compositional driven changes of the spin reorientation were observed. Ordered alloy monolayers were found for GdFe_2/W(110) [8] and NiMn on Ni(111) [9]. Pierce *et al.* [10] observed for $\mathrm{Co}_x\mathrm{Fe}_{1-x}$ alloy nanowires grown on a vicinal W(110) surface that Co frustrates ferromagnetic order unlike the bulk behavior. In their study, however, a phase separation between Fe and Co as well as an influence of the nanowire configuration could not be excluded. Phase separation due to epitaxial stress has been described theoretically [11] and observed experimentally [12,13]. Thus, it has to be taken into account for all studies on alloy films even when the elements are completely miscible in the bulk.

The $\mathrm{Co}_x\mathrm{Fe}_{1-x}$system is particularly interesting, because bulk Co-Fe alloys show the largest magnetization (for $x = 0.3$) of all binary alloys [14]. For $x < 0.25$, the Curie temperature T_C is below the bcc to fcc structural phase transition temperature and increases with increasing x [15]. For $0.25 \leq x < 0.7$, the structural phase transition coincides with T_C. A mean field model preserving the bcc structure reveals a large maximum in the "virtual" T_C for $x = 0.5$ [16]. Co and Fe are continuously miscible. The equiatomic alloy forms an ordered alloy (CsCl) below 1000 K [15].

In this Letter, we show that in $\mathrm{Co}_x\mathrm{Fe}_{1-x}$/W(110) monolayers Fe and Co are indeed miscible. The atomic positions of Fe and Co are characterized by scanning tunneling microscopy (STM) and low energy electron diffraction (LEED) revealing a new short range ordered CoFe_3 structure in addition to the CoFe structure known from the bulk behavior [15]. The decrease of T_C with increasing Co concentration observed in Ref. [10] is observed for monolayers grown on a flat W(110) surface and for Au covered monolayers also. Moreover, from magnetic properties of thicker $\mathrm{Co}_x\mathrm{Fe}_{1-x}$/W(110) alloy films, we find evidence that the frustration of ferromagnetic order with increasing Co concentration is a ground state property of the pseudomorphic (ps) $\mathrm{Co}_x\mathrm{Fe}_{1-x}$/W(110) monolayer system.

Experiments were performed in ultrahigh vacuum with a base pressure of 8×10^{-11} Torr. The tungsten crystal was cleaned as described previously [17]. We use a W(110) crystal with a flat and a vicinal surface (steps parallel to the [100] direction with a mean distance of 9.1 nm) to compare structural and magnetic properties for extended monolayers and nanowires, which were prepared in the step flow growth mode. Fe and Co (99.99% purity) were deposited simultaneously from BeO crucibles. The evaporation rate was monitored by a quartz balance which in turn was calibrated by STM images of pure element coverages $\Theta \leq 0.5$ where pseudomorphic growth is warranted from previous investigations [18,19] for both elements. $\Theta = 1$ corresponds to the coverage of one ps monolayer. In addition to samples of homogeneous composition, we prepared samples with a linearly varying

0031-9007/03/90(7)/077201(4)$20.00

composition profile (4 mm width) and homogeneous coverage using a two shadowmask technique. Magnetic properties were investigated by Kerr magnetometry (wavelength of light 670 nm) described in Ref. [7].

$Co_xFe_{1-x}/W(110)$ submonolayers form islands when deposited at $T_d = 300$ K and grow in the step flow growth mode at $T_d = 700$ K, similar to pure Fe films [7]. An intermediate temperature (400 K) is the optimum temperature for the growth of ordered alloy structures as shown by electron diffraction (LEED). For $x < 0.5$, the alloy monolayer appears as a homogeneous atomic layer for STM images with lower resolution [Figs. 1(a) and 1(b)], whereas for $x > 0.5$ phase separations occur [Fig. 1(c)]. Atomically resolved STM images reveal a $CoFe_3$-$p(2 \times 2)$ [20] [Fig. 1(d)] and CoFe-$c(2 \times 2)$ [Fig. 1(e)] ordered alloy structure for Fe rich alloys. Within the phase separated island, we found a close-packed (cp) structure in Nishiyama-Wassermann (NW) orientation [21], similar to the growth of pure Co on W(110) [19] [Fig. 1(f)], which indicates that the separation consists of a Co rich alloy. LEED provides better statistical information. In addition to the (1×1) spots observed for pure Fe films, we observed a $p(3 \times 2)$ superstructure for $x \leq 0.1$, which was not found by STM, and a $p(2 \times 2)$ (for $0.1 < x < 0.5$) and $c(2 \times 2)$ (for $0.3 < x < 0.8$) superstructure, related to the real space images shown in Figs. 1(d) and 1(e). Superstructure spots corresponding to the NW structure are observed for $0.6 < x \leq 1.0$. At $T_d = 700$ K or after annealing at 700 K, the $p(2 \times 2)$ and $c(2 \times 2)$ superstructure spots become very broad, indicating a short range order of a few unit cells only, while the (1×1) diffraction spots remain sharp, confirming the ps structure. The monolayer structure for $x < 0.6$ thus corresponds to a freezed random alloy structure.

Figure 2 shows magnetic properties of a Co_xFe_{1-x} concentration wedge with a fixed coverage of $\Theta = 0.7$, covered by 5 ML of Au. The Co_xFe_{1-x} submonolayer was prepared at 700 K in order to ensure a step flow growth mode, which was checked by STM. The Au coverage, which is known to increase T_C for extended Fe/W(110) monolayers [22] was deposited at 300 K to prevent any interdiffusion and serves as a protection for residual gas adsorption. Magnetic properties were determined from easy-axis magnetization loops, measured for the field applied along $[1\bar{1}0]$. T_C, defined as the temperature where the remnant Kerr rotation vanishes, decreases with increasing Co concentration for extended alloy monolayers grown on the flat W(110) surface as well as for nanostripes formed on the vicinal surface. The nanostripe structure leads to a lower value of T_C compared to extended monolayers for all Co concentrations, similar to the behavior of pure Fe nanostripes observed previously [17,23]. This is attributed to the reduced dimensionality of the quasi-one-dimensional nanostripes formed on the vicinal surface as has been extensively discussed in Ref. [17]. The remnant Kerr rotation measured at the lowest available temperature (93 K) decreases with increasing Co concentration, and vanishes at $x = 0.5$. Similar data for extended monolayers could not be obtained because of the increase of the coercive force at low temperatures. Our results for the Au coated nanostripes agree nicely to the results reported in Ref. [10]. From the coincidence of the decrease of T_C for nanostripes and extended monolayers, we conclude that this behavior is an intrinsic property of the $Co_xFe_{1-x}/W(110)$ system and not induced by the nanostripe geometry. It is also not

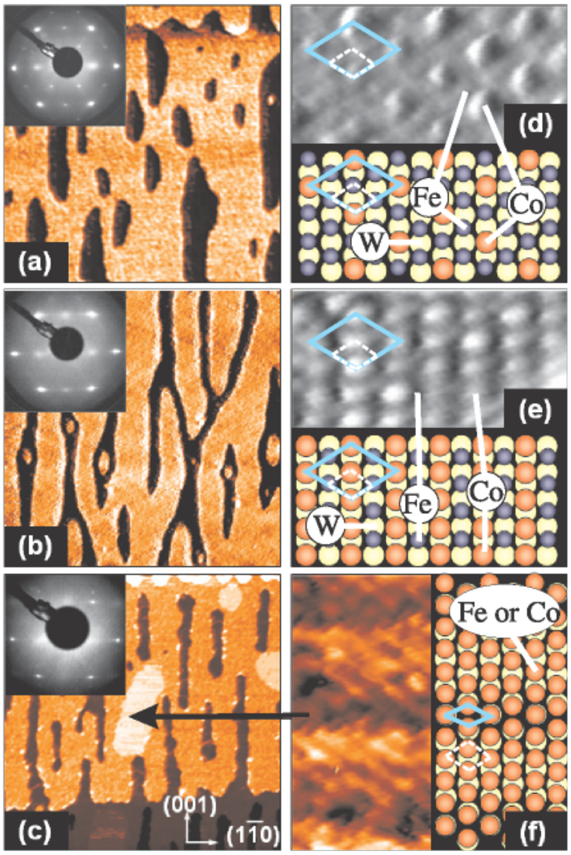

FIG. 1 (color online). STM images (100 nm × 100 nm) of $Co_xFe_{1-x}/W(110)$ pseudomorphic (ps) submonolayers grown at 400 K, coverage $\Theta = 0.7$, for $x = 0.3$ (a), $x = 0.4$ (b), and $x = 0.6$ (c). Bright areas correspond to a monolayer coverage, black areas indicate the W(110) substrate. The island indicated by an arrow in (c) is a close-packed Co-rich segregation, which occurs for all compositions $x > 0.5$. The insets show the LEED images taken at 80, 110, and 170 eV, respectively, from the same samples. The STM images with atomic resolution were taken from nominal compositions $x = 0.3$ [(d) and (e)] and $x = 0.6$ (f), and show a $CoFe_3$-$p(2 \times 2)$ structure (d) corresponding to the LEED image shown in (a), a CoFe-$c(2 \times 2)$ structure (e) corresponding to the LEED image shown in (b), and a cp structure (f) taken at the site indicated by the arrow in (c). Corresponding structure models and rhombohedric unit cells for substrate potential minima (dashed line) and Fe/Co (full line) are indicated in (d)–(f).

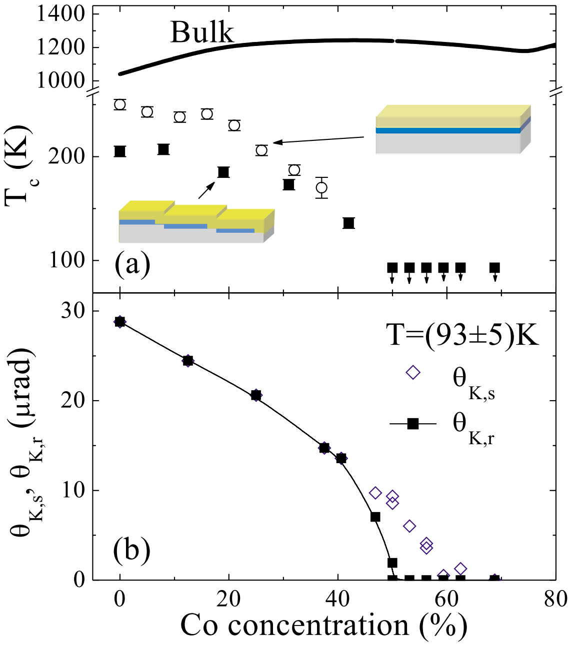

FIG. 2 (color online). (a) Dependence of the T_C on the Co concentration of a Co_xFe_{1-x} submonolayer ($\Theta = 0.7$) grown in the step flow growth mode on flat and stepped W(110) at 700 K and covered by 5 ML Au at 300 K. T_C values that correspond to the last data points must lie below the temperature shown. Data for bulk Co-Fe alloys [15] are given for comparison. (b) Dependence of the remnant and saturation Kerr rotation, $\theta_{K,r}$ and $\theta_{K,s}$, on the Co concentration measured at the lowest achievable temperature for the same sample on the stepped side of the crystal.

caused by a phase separation of Fe and Co as can be concluded from our structural analysis described above. However, it could be caused by a spin reorientation transition or by a drastic increase of the coercive force with increasing Co concentration [24,25].

In order to exclude these extrinsic explanations, we prepared alloy films in the thickness range 1.8–6 ML. The films were deposited at 300 K providing the best approximation to a layer by layer growth in this thickness regime. For pure Fe/W(110) films, it was proven by Mössbauer spectroscopy [18] that the first monolayer attached to the substrate stays in the ps state even for thicker films, while additional Fe grows in (110) orientation with almost bulk lattice structure. The same growth mode can be expected for Co_xFe_{1-x} alloy films. The sample corresponds to a ps Co_xFe_{1-x}/W(110) monolayer covered by a ferromagnetic coating with a T_C value close to the bulk value and a constant easy axis along $[1\bar{1}0]$. Because of the strong ferromagnetic exchange coupling, ferromagnetic components of the first ps layer will be polarized along the mean magnetization direction.

We observed easy-axis magnetization loops at 300 K for the external field applied along $[1\bar{1}0]$ for all samples. For constant Co concentration x, the remnant Kerr rotation $\theta_K(x, D)$ increases linearly with the thickness D (measured in numbers of atomic layers with bulk structure):

$$\theta_K(x, D) = \theta_K(x, 1)[D + D_0(x)], \tag{1}$$

similar to the behavior observed for pure Fe films [26] (see Fig. 3). While the specific Kerr rotation per monolayer $\theta_K(x, 1)$ shows the well-known bulk behavior [27], the interface induced contribution $D_0(x)$ decreases considerably with x for small Co concentration and reaches a minimum of $D_0(0.6) = -1.05$ ML. $\theta_K(x, 1)$ is almost independent of temperature below 300 K because the bulk magnetization shows a minor variation of only a few percent. $D_0(x)$ is composed of the true ground state contribution (surface effect) and the temperature dependent size effect $D_{size}(T)$, which describes the enhanced temperature dependence of magnetic order in thin films: $D_0(x) = D_{surf}^{CoFe/W} + D_{surf}^{CoFe/UHV} + D_{size}(T)$ [26]. The size effect for Fe/W(110) and Co/W(110) films $D_{size}(300\text{ K}) = -0.5$ ML was determined previously for both elements [26,28] and a similar value can be expected for the alloy. The surface effect of the free Fe and Co surface exposed to UHV is positive, reflecting an enhanced magnetization at the free surface. It has been measured for Fe(110), $D_{surf}^{Fe/UHV} = +0.4$ ML [26], and determined by a theoretical calculation for Co(0001), $D_{surf}^{Co/UHV} = +0.07$ ML [29]. There is no reason why the magnetization at the alloy surface should deviate from these values considerably. We conclude that the size effect and the surface effect of the free surface partly compensate each other and that the main contribution to the observed large negative values of $D_0(x)$ near $x = 0.5$ is attributed to the surface effect at the tungsten interface.

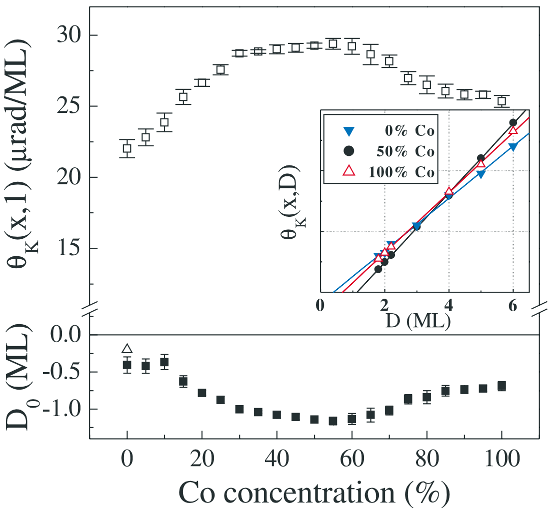

FIG. 3 (color online). Dependence of the specific Kerr rotation per monolayer $\theta_K(x, 1)$ and the interface contribution D_0 on the Co concentration, determined by linear fits of $\theta_K(x, D)$, as shown exemplarily in the inset.

Assuming a linear interpolation between the size effect and the surface effect of the free surface for Fe and Co films, we obtain $D_{\mathrm{surf}}^{\mathrm{CoFe/W}} = -0.7(1)$ ML, which corresponds exactly to the frustration of ferromagnetic order in the ps CoFe/W(110) monolayer. The cp Co-rich phases formed at the tungsten interface for $x \geq 0.6$ can appearingly be polarized, which would explain the increase of $D_0(x)$ for $x \geq 0.6$.

As a result of the $3d$ electron states, the existence of ferromagnetic order is related to whether the Stoner criterion $IN(E_F) > 1$ is fulfilled or not, where $N(E_F)$ is the density of states (DOS) at the Fermi level (E_F) in the paramagnetic phase, and I denotes the Stoner parameter which is an intra-atomic quantity and is known to depend only little on crystal environment [1]. The Stoner criterion states that ferromagnetism appears when the gain in exchange energy is larger than the loss in kinetic energy. *Ab initio* band structure calculations reveal that in bulk (bcc) Fe the electron states in the paramagnetic phase are filled up before the maximum of the DOS is reached [1]. For small Co concentrations, the band structure is not changed except for an increasing d-band filling. An increasing band filling with increasing Co concentration then leads to an increase of $N(E_F)$, thus explaining the increase of T_C observed for bulk CoFe alloys. For an Fe/W(110) monolayer, instead, E_F is shifted to a higher energy and is placed beyond the maximum of the DOS [30]. An increasing band filling then would lead to a decrease of $N(E_F)$ and as a consequence of the Stoner model decrease T_C, which is observed in our experiment.

Although the magnetization is not proportional to the Kerr rotation, the specific Kerr rotation varies only little with x. Therefore, we take the Kerr rotation as a rough measure for the magnetization. The decrease of magnetization at low temperatures observed for $\mathrm{Co}_x\mathrm{Fe}_{1-x}$/W(110) monolayers with increasing x might be attributed to a filling of d holes, similar to the properties of alloys on the right branch of the Slater-Pauling curve. The initial reduction of the Kerr rotation with increasing x corresponds to a reduction of $\Delta\mu = 2.9\mu_{\mathrm{B}}$ per additional d electron (assuming a ground state moment of $2.5\mu_{\mathrm{B}}$ per atom for the Fe/W(110) monolayer [31]). This is in sharp contrast to the Slater-Pauling behavior of $\Delta\mu = 1\mu_{\mathrm{B}}$ per electron.

In summary, we prepared a quasi-two-dimensional ferromagnetic alloy and observed short range ordered CoFe_3 and CoFe structures. Magnetization and T_C decrease with increasing Co concentration. The decrease of T_C can be explained by the Stoner model, modified for $\mathrm{Co}_x\mathrm{Fe}_{1-x}$/W(110) monolayers. Quasi-one-dimensional alloy nanostripes formed on the vicinal surface show reduced values for T_C.

We gratefully acknowledge financial support from the Deutsche Forschungsgemeinschaft.

[1] P. James, O. Eriksson, B. Johansson, and I. A. Abrikosov, Phys. Rev. B **59**, 419 (1999).

[2] F. O. Schumann, R. F. Willis, K. G. Goodman, and J. G. Tobin, Phys. Rev. Lett. **79**, 5166 (1997).

[3] A. Dittschar, W. Kuch, M. Zharnikov, and C. M. Schneider, J. Magn. Magn. Mater. **212**, 307 (2000).

[4] F. Matthes, M. Seider, and C. M. Schneider, J. Appl. Phys. **91**, 8144 (2002).

[5] S. D. Bader, Surf. Sci. **500**, 172 (2002).

[6] *Ultrathin Magnetic Structures*, edited by J. A. C. Bland and B. Heinrich (Springer-Verlag, Berlin, 1992), Vols. I and II.

[7] H. J. Elmers, Int. J. Mod. Phys. B **9**, 3115 (1995).

[8] R. Pascal, M. Getzlaff, H. Tödter, M. Bode, and R. Wiesendanger, Phys. Rev. B **60**, 16109 (1999).

[9] M. A. J. Allen and D. Venus, Surf. Sci. **477**, 209 (2001).

[10] J. P. Pierce, E.W. Plummer, and J. Shen, Appl. Phys. Lett. **81**, 1890 (2002).

[11] G. Abadias, A. Marty, and B. Gilles, Acta Mater. **46**, 6403 (1998).

[12] S.-J. Kahng, Y. J. Choi, J.-Y. Park, and Y. Kuk, Appl. Phys. Lett. **74**, 1087 (1998).

[13] S. Krimmel, W. Donner, B. Nickel, H. Dosch, C. Sutter, and G. Grubel, Phys. Rev. Lett. **78**, 3880 (1997).

[14] R. M. Bozorth, *Ferromagnetism* (Van Nostrand, New York, 1951).

[15] T. Nishizawa and K. Ishida, *Binary Alloy Phase Diagrams* (ASM, Materials Park, OH, 1986), Vol. 1, p. 764.

[16] J. M. MacLaren, T. C. Schulthess, W. H. Butler, R. Sutton, and M. McHenry, J. Appl. Phys. **85**, 4833 (1999).

[17] J. Hauschild, H. J. Elmers, and U. Gradmann, Phys. Rev. B **57**, R677 (1998).

[18] M. Przybylski, I. Kaufmann, and U. Gradmann, Phys. Rev. B **40**, 8631 (1989).

[19] H. Knoppe and E. Bauer, Phys. Rev. B **48**, 1794 (1993).

[20] The relation between the surface and substrate lattice is expressed by the ratios of the lengths of the basis vectors. The unit cell may either be primitive (p) or centered (c).

[21] J. H. van der Merwe, Philos. Mag. A **45**, 145 (1982).

[22] U. Gradmann, G. Liu, H. J. Elmers, and M. Przybylski, Hyperfine Interact. **57**, 1845 (1990).

[23] M. Pratzer, H. J. Elmers, M. Bode, O. Pietzsch, A. Kubetzka, and R. Wiesendanger, Phys. Rev. Lett. **87**, 127201 (2001).

[24] H. J. Elmers, J. Hauschild, H. Fritzsche, G. Liu, U. Gradmann, and U. Köhler, Phys. Rev. Lett. **75**, 2031 (1995).

[25] D. Sander, R. Skomski, C. Schmidthals, A. Enders, and J. Kirschner, Phys. Rev. Lett. **77**, 2566 (1996).

[26] K. Wagner, N. Weber, H. J. Elmers, and U. Gradmann, J. Magn. Magn. Mater. **167**, 21 (1997).

[27] G. A. Prinz, W. G. Maisch, P. Lubitz, D.W. Forrester, and J. J. Krebs, IEEE Trans. Magn. **17**, 3232 (1981).

[28] H. Fritzsche, Ph.D. thesis, Technical University of Clausthal, Germany, 1995.

[29] C. Li, A. J. Freeman, and C. L. Fu, J. Magn. Magn. Mater. **94**, 134 (1991).

[30] X. Qian and W. Hübner, Phys. Rev. B **60**, 16192 (1999).

[31] H. J. Elmers, G. Liu, and U. Gradmann, Phys. Rev. Lett. **63**, 566 (1989).